TAF
Journal of Advances in Technology and Engineering Research
JATER
2021, **7**(1): 17-24

PRIMARY RESEARCH

Comparation of Shell Thickness Integration Rules and Element Types on Single Point Incremental Forming (SPIF) Simulation

Chen Wenning[1*], Li Sijia [2], Krishna Singh Bhandari [3], Kosimov Nodirbek [4], Dongwon Jung[5]
[1, 2, 3, 4, 5] Department of Mechanical Engineering, Jeju National University, Jeju Island, South Korea

Keywords
SPIF
Numerical simulation
Element type
Explicit analysis Shell element

Received: 12 February 2021
Accepted: 09 April 2021
Published: 7 June 2021

Abstract
As a new rapid prototyping technology, Single Point Incremental Forming (SPIF) gains considerable investigation and development as its simple manufacturing tools, low cost, etc. To predict the quality of the manufacturing finished products and reduce experimental costs, many scholars and companies applied and investigated numerical simulation of SPIF. However, many problems emerge like extremely long simulation time, difficulties in forecasting profile geometry and thickness variation, etc. A long way needs to explore to improve the accuracy of SPIF simulation. Focus on this target, and this paper studied the influences of shell thickness integration rules (Simpson and Gauss), sheet thickness, and element types (with reduction and full reduction) on simulation accuracy. For the experiment, a top diameter of 115 mm, bottom diameter of 12mm, and 27 mm high cone part was formed on a customized three-axis CNC milling machine. Contourgraph was used to obtain profile geometry. Then the deformed part was cut, and a micrometer was used to obtain thickness distribution along with the profile of the formed sheet, respectively. For simulation, shell elements were employed to simulate SPIF explicit simulation. Furthermore, Simpson and Gauss rules integral in thickness direction were used for simulating the same geometry part, and the results were compared. Average Absolute Relative Error (AARE) was used to compare all the profiles and thickness from simulations and experiments, and it can be found that element types with reduction integration can get more accurate results and cost less time. Furthermore, the Gauss integration rule along shell thickness is more accurate than the Simpson rule. Therefore, to achieve greater accuracy, it is recommended to use the Gauss integration rule and reduction integration element (S4R) to predict the profile geometry and thickness prediction in SPIF dynamic explicit simulation.

I. INTRODUCTION

Origin from 1978 Mason's work that forms small batch parts by using a single spherical tool to move along three coordinates (x, y, z) [1], SPIF has attracted many researchers to conduct research and develop more diversified for decades. The basic manufacturing form of SPIF is that the target sheet is fixed with four edges on the machine platform, with the spherical tool moving along the sheet surface and moving down along Z-axis in little increments by following the NC code generated by manufacturing software, the final geometry of the part is forming gradually [2, 3], see Fig. 1. Because of the advantage that SPIF can be conducted on a three-axis CNC milling machine, many scholars can investigate it as long as this condition is met.

Many works were done on SPIF, and many kinds of parts were formed. In the field of kitchenware. Jeswiet et al. [4] manufactured a customized solar oven for developed countries, which high accuracy is not required and produced with less money; Also, SPIF is used in the medical supplies. Micari [5] proposed the technological circulation process of scanning, modeling, shape embedding, and manufacturing ankle support produced by SPIF. Skull implants were made by Duflou et al. [6] with a whole manufacturing process based on SPIF, and many scholars have recognized this

*Corresponding author: Chen Wenning
†email: chenwnxy98@stu.jejunu.ac.kr

application as potentially feasible. SPIF is widely used in automobile manufacturing for shell production. SPIF was adopted by Amino et al. [7] to produce replacement parts for cars.

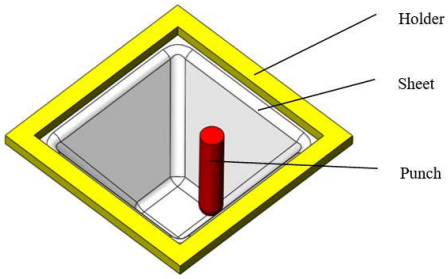

Fig. 1. Process principles of SPIF

With the high accuracy of results and rapid development of computing power, numerical simulation technology has been greatly developed and adopted in many fields; SPIF is no exception. The two main methods people use to simulate SPIF are implicit and explicit dynamic simulations. Due to the implicit dynamic method involves iterative convergence and explicit dynamic does not consider it but relies on the maximum natural frequency of the model [8, 9], explicit dynamic calculates faster than implicit. However, the implicit calculation results are more accurate than explicit (especially in sheet thickness and profile geometry prediction). He et al. [10] employed implicit and explicit ways to simulate incremental forming. They found that the time consumption of implicit simulation is four times that of explicit, but the result showed that explicit thickness results oscillate near the experiment value and implicit keep good consistency with the experiment value. The same work was also done by Tamer et al., [11] and they simulated cone, pyramid, and auto-body parts. The results show that simulations executed by implicit dynamic simulation have better geometric accuracy and strain accuracy, but explicit algorithm takes less time and the errors is within the acceptable range.

Under comprehensive consideration, explicit dynamic method seems a better way to carry out SPIF simulation. However, there are many noteworthy issues occurs during explicit dynamic simulation. Like, accuracy lost in thickness and spring back prediction [12]. Many factors affect the simulation accuracy like element types, integral rules, etc. To determine a better parameter lection to carry on SPIF simulation in explicit dynamic way, this paper implement simulation in Simpson and Gauss thickness integration rules. And for mesh types, shell element with reduction (S4R) and shell element with full reduction (S4) was adopted to make comparation with experimental profile geometry and thickness distribution.

II. MATERIALS AND METHODS

The material used in this paper is aluminum alloy AA3003-H18; Table 1 shows the chemical composition of Al AA3003-H18. The stress-strain curve of Al AA3003-H18 was obtained by tensile test, and mechanical properties were summarized in Table 2. In the Simulation part, mechanical properties and stress-strain curves are needed to define the material properties.

TABLE 1
CHEMICAL COMPOSITION OF AL AA3003-H18

Composition	Al	Mn	Fe	Si	Cu	Zn
wt%	96.7-99.1	1.0-1.5	0.7	0.6	0.05-0.20	0.1

TABLE 2
MECHANICAL PROPERTIES OF AL AA3003-H18

Parameters		Units
Density	2730	Kg/m^3
Elasticity Modulus	69.581	Gpa
Poisson's ratio	0.33	
Yield stress	164.088	Mpa
Ultimate tensile stress	192.878	Mpa
Total elongation (%)	4.948	
Anisotropy factor (r)	1.126	
Strain hardening exponent (n)	0.125	
Hardening coefficient (k)	335.665 Mpa	
Average strain hardening exponent (n)	0.117	
Average hardening coefficient (k)	346.707 Mpa	

ISSN: 2414-4592
DOI: 10.20474/jater-7.1.3

The main integration method of simulation software is Gauss integration rule. For two-dimension questions, Gauss integration can be written as:

$$I = \int_{-1}^{1}\int_{-1}^{1} f(\xi,\eta)d\xi d\eta = \sum_{i,j=1}^{n} A_{ij} f(\xi_j,\eta_i) \quad (1)$$

While $A_{ij} = A_i A_j, \xi_j, \eta_i$ are integration points of one-dimension Gauss integration, A_i, A_j are integration weight coefficient.

The integration points of different element types are different. The order of Gauss integration is related to the highest power term of interpolation function. An integration scheme in which the order of the Gauss integration is the same as the order required for all the exact integrations of the integrand is called full integration. An integration scheme that is lower than the order required for the exact integration of all terms of the product is called reduction integration [13]. Fig. 2 shows the integration point location of S4R shell element.

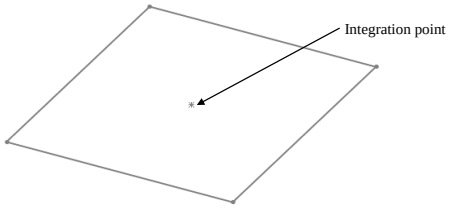

Fig. 2. Integration point location of S4R shell element

In thickness integration Simpson and Gauss rules were adopted, formulas are as follows:

$$\text{Simpson:} I = \int_a^b f(x)dx = \frac{b-a}{6n}\left[y_0 + y_{2n} + 4\left(y_1 + y_3 + \cdots + y_{2n-1}\right) + 2\left(y_2 + y_4 + \cdots + y_{2n-2}\right)\right] \quad (2)$$

$$\text{Gauss: } I = \int_{-1}^{1} f(\xi)d\xi = \sum_{i=1}^{n} A_i f(\xi_i) \quad (3)$$

Integration points are evenly distributed in the thickness direction. See Fig. 3.

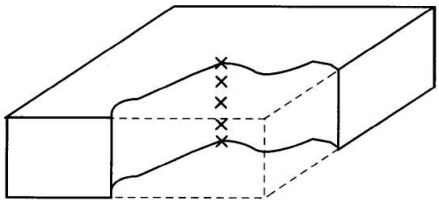

Fig. 3. Distribution of integration points in shell section (five integration point)

In order to accurately determine the similarity of profile geometry and thickness distribution between simulation and experiment, AARE was employed. Scatter points equidistantly on the section of the experimental formed part, keep point numbers consistent with the integration points of simulation profile. By comparing the relative error one by one, AARE can be realized by following expression:

$$\text{AARE} = \frac{1}{n}\sum_{i=1}^{n}\left|\frac{x_{\text{exp}}^{i} - x_{\text{Sim}}^{i}}{x_{\text{exp}}^{i}}\right| \times 100\%$$

Where x_{exp} is y-coordinate (for profile comparation) and thickness (for thickness distribution comparation) in each experiment point. x_{sim} is y-coordinate (for profile comparation) and thickness (for thickness distribution comparation) in each simulation integration point.

III. EXPERIMENT

An Al AA3003-H18 sheet 210 mm long, 250 mm wide and 0.55 mm thickness was put under a 6 mm thickness holder. Then they are bolted to the customized three-axis CNC milling machine. See Fig. 4. The target part geometry was formed and generated NC code by commercial modeling and processing software Fusion 360. Then the NC code was transferred to CNC machine. During the forming process, in order to reduce the friction damping between sheet and tool, a lubricant made from a mixture of grease and oil was adopted. Finally, the target geometry part was got and the profile geometry was obtained by a Contourgraph. Then the deformed sheet part was cut in half along middle line to obtain the sheet thickness distribution, which can be seen in Fig. 5.

ISSN: 2414-4592
DOI: 10.20474/jater-7.1.3

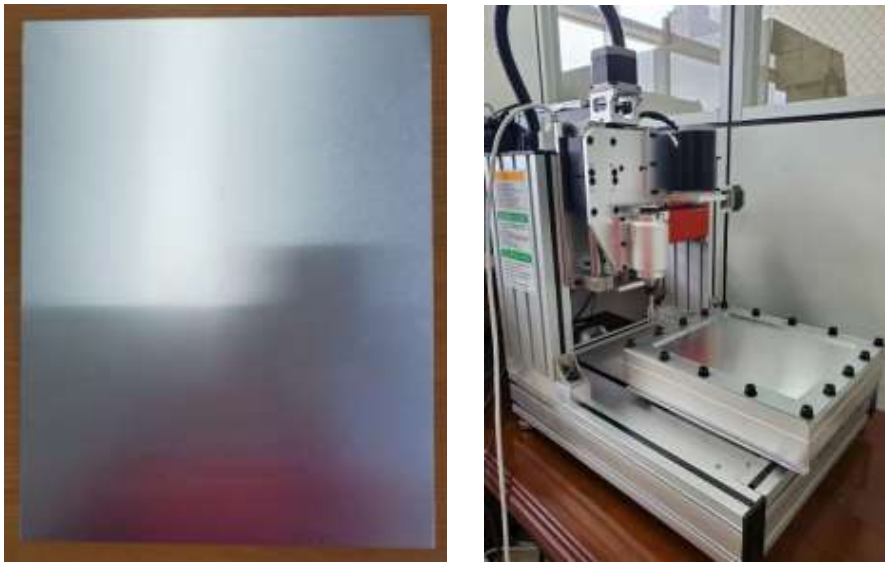

(a) (b)

Fig. 4. Experimental sheet 210 mm × 250 mm (a) and customized three-axis CNC milling machine (b)

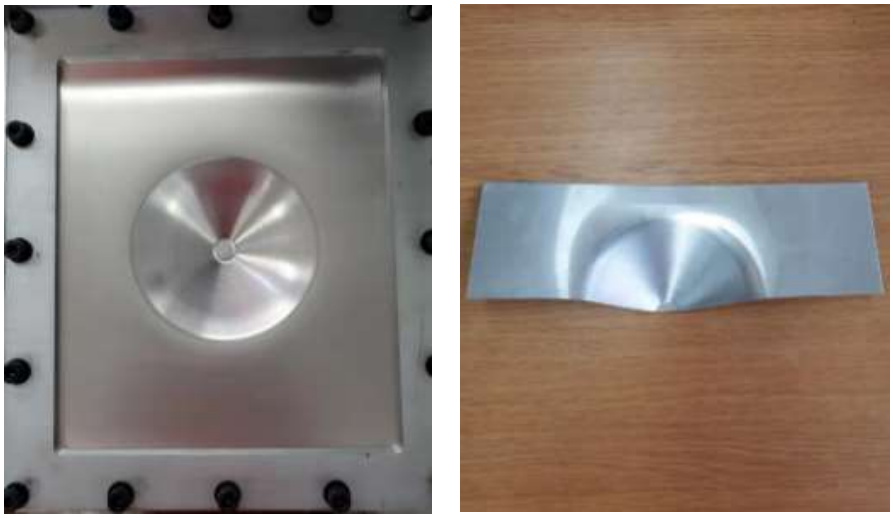

(a) (b)

Fig. 5. Formed sheet part (a) and half part after cutting (b)

IV. NUMERICAL SIMULATION

The model of sheet and punch were imported to the simulation software after modelling by Fusion 360. Material properties were filled according to Table 2, and FLD damage curve was imported for damage prediction. The degrees of freedom in six directions were fixed of four sheet edges were fixed to simulate the initial state of the sheet fixed on the work platform. Because the lubricant was used in the forming process, the tangential behavior was set as penalty, value 0.05. The tool path of punch was transformed from the NC code to x, y, z position coordinates for punch moving in Cartesian rectangular coordinate system during simulation. Although explicit dynamic simulation is shorter than implicit dynamic simulation, the time cost is still long. For this reason, mass scaling was used in the whole for the whole simulation and the mass scaling factor was set as 10000. However, the inertia effect caused by excessive mass scaling will increase the error. To avoid this, an important evaluation index is the kinetic energy and internal energy ratio of sheet should be kept below 5% [14]. In section definition part, the homogeneous, continuum shell was adopted. Set Simpson thickness integration rule and

ISSN: 2414-4592
DOI: 10.20474/jater-7.1.3

Gauss integration rule respectively as comparation and set three integration points in the thickness direction. In meshing part, the first-order interpolation shell element with reduction integration (S4R) and full integration (S4) were adopted as comparation. Fig. 6 shows the molded sheet and formed sheet during numerical simulation process.

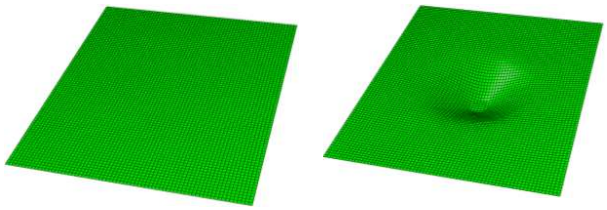

(a) (b)

Fig. 6. Initial sheet model (a) and deformed sheet model (b) during simulation

V. RESULTS

Four simulation results (Simpson+S4R, Simpson+S4, Gauss+S4R, Gauss+S4) and experiment result were obtained to compare profile geometry and thickness distribution. As can be seen in Fig. 7, the region beside formed region sinks and this region is also the region with the largest deviation. The experimental sink region is deeper than simulation. What's more, the middle region of bottom is higher than bottom edge region. Simpson+S4 simulation has a visible deviation from other simulations and experiment. Fig. 8 shows thickness distributions, the areas with serve deformation are the areas in direct contact with the punch. The thinning in other areas is not obvious.

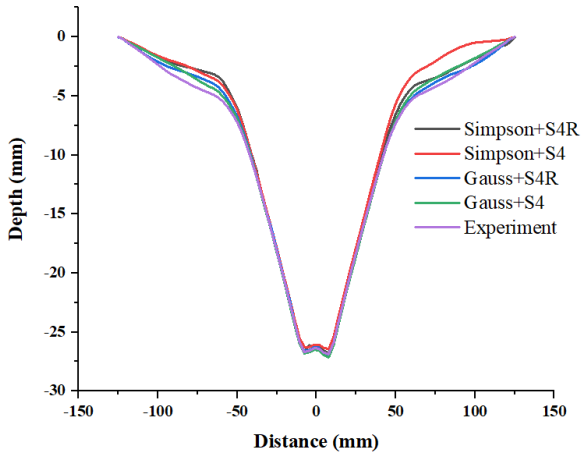

Fig. 7. Profile geometries of simulations and experiment

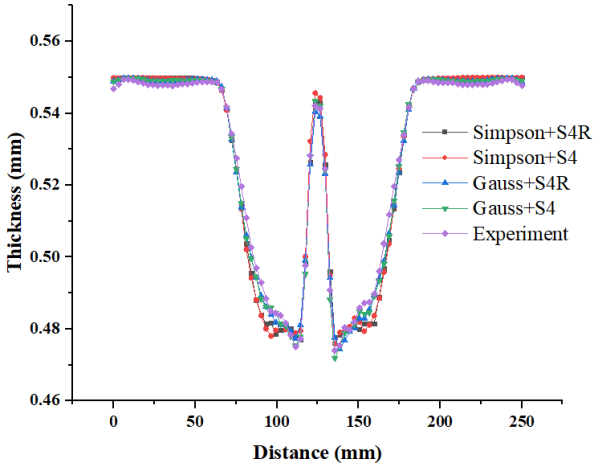

Fig. 8. Thickness distribution along the deformed sheet profile

AARE was used to get quantitative simulation error. As can be seen in Table 3, Gauss integration rule can get better accuracy than Simpson integration rule, especially in profile geometry prediction. For thickness distribution, simulation always keep very low AARE, so shell section can accurately predict thinning. Table 4 shows the simulation time cost of four comparation simulation, it is not difficult to find that element with reduction cost less simulation time.

ISSN: 2414-4592
DOI: 10.20474/jater-7.1.3

TABLE 3
AARES OF SIMULATIONS

	Simpson+S4R	Simpson+S4	Gauss+S4R	Gauss+S4
Profile geometry	16.93%	27.67%	6.67%	9.96%
Thickness	0.48%	0.51%	0.31%	0.25%

TABLE 4
SIMULATION TIME COST OF SIMULATIONS

	Simpson+S4R	Simpson+S4	Gauss+S4R	Gauss+S4
Simulation time cost (Sec)	26845	99130	25863	99554

In order to make sure the influence of inertia effect produced by mass scaling setting, the ratios of kinetic energy and internal energy were obtained, see Fig. 9. The maximum value of kinetic energy/Internal energy ratios is 1.4% (under 5%), all simulation results are reliable consequently.

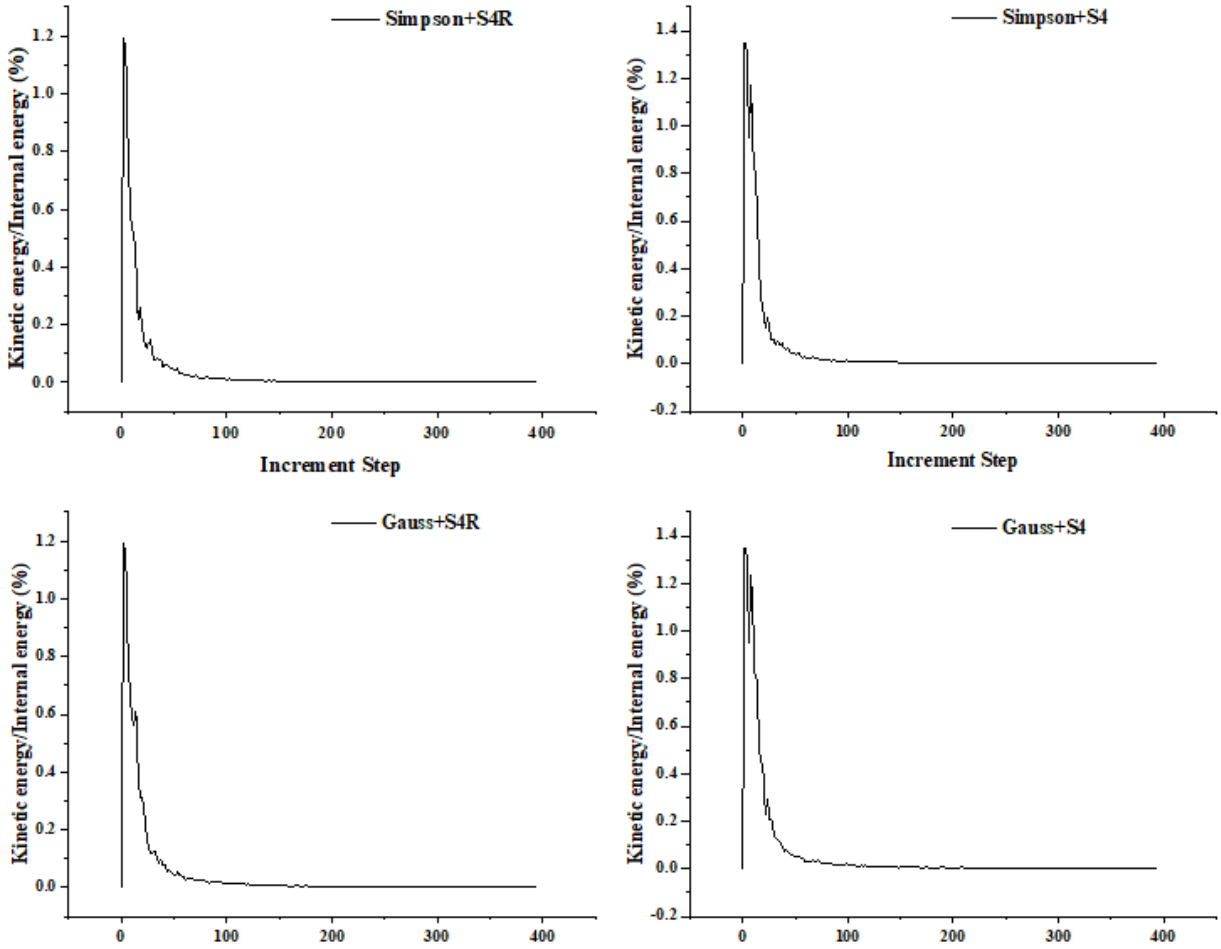

Fig. 9. Kinetic energy and internal energy ratio of four simulation settings

VI. DISCUSSION

According to results comparation, it can be found that shell elements in dynamic explicit simulation can predict thickness distribution accurately, but has poor ability to predict profile geometry. Gauss integration along thickness possesses higher accuracy than Simpson integration rule. In addition, reduction integration element does better than full integration element in profile geometry reduction. The AARE of Simpson integration rule along thickness with S4 element is up to 27.67%. By change the thick-

ISSN: 2414-4592
DOI: 10.20474/jater-7.1.3

ness integration rule and element type, AARE reduced to 6.67% (Simpson+S4R). Although Gauss+S4 behaves better than Gauss+S4R in thickness distribution prediction, it's improvement in accuracy is minimal (only 0.06%). What's more, the simulation time cost of full integration element is 3.8 times as much as reduction integration element. On the contrary, the integration rules in thickness direction have little effect on simulation time. In summary, whether in terms of accuracy or simulation time cost, the scheme Gauss+S4R is the optimal solution.

VII. CONCLUSION

Based on the explicit dynamic simulation requires less simulation time without losing much accuracy than implicit dynamic simulation, many factors need to intensive study on the impact on the accuracy of results during explicit dynamic simulation. Shell thickness integration rule and shell element type are two of them. In order to study this question, a cone part was formed on a customed CNC milling machine and four simulations used shell section in different thickness integration rules and element types (Simpson rule + reduction integration element(S4R), Simpson rule + full integration rule(S4), Gauss rule + reduction integration element(S4R), Gauss rule + full integration rule(S4)) were conducted. Finally, the profile geometries and thickness distributions of experiment and simulations were obtained and analyzed. Conclusions were got as follows:

1. By comparing the AAREs of all simulations, it can be found that the simulation results obtained by Gauss integration in the direction of shell thickness are more accurate than Simpson integration.
2. Shell elements have a high ability to predict sheet thinning for SPIF simulation, but poor ability in predicting profile geometry. However, comparing with Simpson thickness integration rule with full integration element (S4), by adopting Gauss thickness integration rule with reduction integration element (S4R), it can improve the accuracy by 21%.
3. Simulations adopted reduction integration element cost 2.8 times less simulation time than full integration element simulation and can get more accurate prediction result. The simulation methods have very small effect on simulation time. Therefore, a strategy that shell thickness integrated by Gauss integration rule with reduction integration element is encouraged to use for SPIF dynamic explicit simulation.

ACKNOWLEDGEMENT

This work was supported by the Korea Institute of Energy Technology Evaluation and Planning (KETEP) grant funded by the Korea government (MOTIE) (20206310100050, A development of remanufacturing technology on the guiding system of complex-function for high-precision).

REFERENCES

[1] B. Mason, ``Sheet metal forming for small batches,'' University of Nottingham, Nottingham, UK, Bachelor thesis, 1978.
[2] W. Emmens, G. Sebastiani, and A. H. van den Boogaard, ``The technology of incremental sheet forming - a brief review of the history,'' *Journal of Materials Processing Technology*, vol. 210, no. 8, pp. 981-997, 2010. doi: https://doi.org/10.1016/j.jmatprotec.2010.02.014
[3] P. Martins, N. Bay, M. Skjoedt, and M. Silva, ``Theory of single point incremental forming,'' *CIRP annals*, vol. 57, no. 1, pp. 247-252, 2008. doi: https://doi.org/10.1016/j.cirp.2008.03.047
[4] J. Jeswiet, J. R. Duflou, A. Szekeres, and P. Lefebvre, ``Custom manufacture of a solar cooker-a case study,'' *Advanced Materials Research*, vol. 6, pp. 487-492, 2005. doi: https://doi.org/10.4028/www.scientific.net/AMR.6-8.487
[5] F. Micari, ``Single point incremental forming: Recent results,'' in *Seminar on Incremental Forming, Cambridge University,* Cambridge, UK, vol. 22, 2004.
[6] J. Duflou, B. Lauwers, J. Verbert, F. Gelaude, and Y. Tunckol, ``Medical application of single point incremental forming: Cranial plate,'' in *Proceeding of the 2nd International Conference on Advanced Research in Virtual and Rapid Prototyping VRAP,* Leiria, Portugal, 2005.
[7] H. Amino, Y. Lu, S. Ozawa, K. Fukuda, and T. Maki, ``Dieless NC forming of automotive service panels,'' in *Proceedings of the conference on Advanced Techniques of Plasticity,* Yokohama, Japan, 2002.
[8] D.-Y. Yang, D. Jung, I. Song, D. Yoo, and J. Lee, ``Comparative investigation into implicit, explicit, and iterative implicit/explicit schemes for the simulation of sheet-metal forming processes,'' *Journal of Materials Processing Technology*, vol. 50, no. 1-4, pp. 39-53, 1995. doi: https://doi.org/10.1016/0924-0136(94)01368-B
[9] F. Maqbool and M. Bambach, ``Dominant deformation mechanisms in Single Point Incremental Forming (SPIF) and their effect on geometrical accuracy,'' *International Journal of Mechanical Sciences*, vol. 136, pp. 279-292, 2018. doi:

https://doi.org/10.1016/j.ijmecsci.2017.12.053

[10] S. He, A. Van Bael, P. Van Houtte, Y. Tunckol, J. Duflou, C. Henrard, C. Bouffioux, and A. Habraken, ``Effect of FEM choices in the modelling of incremental forming of aluminium sheets,'' in *Proceedings of the 8th ESAFORM Conference on Material Forming,* Cluj-Napoca, Romania. The Publishing House of the Romanian Academy, 2005.

[11] M. Tamer, O. Music, I. Ozdemir, B. Baranoglu, A. Sakin, and I. Durgun, ``Simulation for incremental sheet forming process: A comparison of implicit and explicit finite element analysis with experimental data,'' in *7th International Conference and Exhibition on Design and Production of Machines and Dies/Molds,* Antalya, Turkey, 2013.

[12] J. Jeswiet, F. Micari, G. Hirt, A. Bramley, J. Duflou, and J. Allwood, ``Asymmetric single point incremental forming of sheet metal,'' *CIRP Annals*, vol. 54, no. 2, pp. 88-114, 2005. doi: https://doi.org/10.1016/S0007-8506(07)60021-3

[13] O. Zienkiewicz, R. Taylor, and J. Too, ``Reduced integration technique in general analysis of plates and shells,'' *International Journal for Numerical Methods in Engineering*, vol. 3, no. 2, pp. 275-290, 1971. doi: https://doi.org/10.1002/nme.1620030211

[14] Z. Zhuo, *Finite element analysis and application on ABAQUS*. Beijing, China: Tsinghua University Press, 2009.

ISSN: 2414-4592
DOI: 10.20474/jater-7.1.3